XII International Conference on Computational Plasticity. Fundamentals and Applications
COMPLAS XII
E. Oñate, D.R.J. Owen, D. Peric and B. Suárez (Eds)

3D NUMERICAL MODEL OF A CONFINED FRACTURE TESTS IN CONCRETE

O. MONTENEGRO[1], D. SFER[2], C.M. LÓPEZ[1] AND I.CAROL[1]

[1]Department of Geotechnical Engineering and Geo-Sciences
ETSECCPB (School of Civil Engineering)-UPC (Technical Univ. of Catalonia), 08034 Barcelona
[2]Universidad Nacional de Tucumán, Argentina
E-mail: oscar.montenegro@upc.edu, sfer@herrera.unt.edu.ar, carlos.maria.lopez@upc.edu, ignacio.carol@upc.edu

Keywords: Fracture test, fracture energy, zero-thickness interface elements.

Abstract. The paper deals with the numerical simulation of a confined fracture test in concrete. The test is part of the experimental work carried out at ETSECCPB-UPC in order to elucidate the existence of a second mode of fracture under shear and high compression, and evaluate the associated fracture energy. The specimen is a short cylinder with also cylindrical coaxial notches similar the one proposed by Luong (1990), which is introduced in a large-capacity triaxial cell, protected with membranes and subject to different levels of confining pressure prior to vertical loading. In the experiments, the main crack follows the pre-established cylindrical notch path, which is in itself a significant achievement. The load-displacement curves for various confining pressures also seem to follow the expected trend according to the underlying conceptual model. The FE model developed includes zero-thickness interface elements with fracture-based constitutive laws, which are pre-inserted along the cylindrical ligament and the potential radial crack plane. The results reproduce reasonably well the overall force-displacement curves of the test for various confinement levels, and make it possible to identify the fracture parameters including the fracture energies in modes I and IIa.

1 INTRODUCTION

Mode I fracture in concrete, including the corresponding energy parameter G_F^I are concepts nowadays well established with a number of papers published in the literature. However, mixed mode fracture involving shear and, especially, confined mixed mode fracture under shear-compression, has received much more limited attention. In 1990 Carol and Prat introduced and later developed [1,2] the concept of asymptotic shear–compression mixed mode or mode IIa, in which very high compression across the fracture plane prevents any dilatancy and forces the crack to propagate sensibly straight, cutting through aggregates and matrix. In later conference papers [3,4] a specific experimental program conceived to elucidate the existence of such mode IIa and calibrate the corresponding fracture energy, G_F^{IIa}, were described.

In the current paper, those results are summarized, and attention is focused on on-going numerical studies aiming at the full interpretation of those experimental results.

2 EXPERIMENTAL SETUP AND RESULTS

The simple idea of creating a shear–compression crack that takes place along a pre-determined plane or surface is no trivial task. Previous attempts to modify typical mode-II (Iosipescu-type) notched beams by applying a compression force across the fracture plane often lead to deviation of the crack trajectory to a different orientation with lower level of transversal compression. For this purpose, the authors have developed a confined fracture test setup on the basis of the short cylindrical specimen originally proposed by Luong [5,6], which was modified in three ways: (i) eliminating the original radial cuts of the outer cylinder (ii) assigning a slightly different diameter to the cylindrical notches from the upper and lower faces, and (iii) introducing the specimen in a triaxial cell and subjecting it to different degrees of confinement previous to the shear tests. The specimen geometry and loading conditions are depicted in Figure 1.

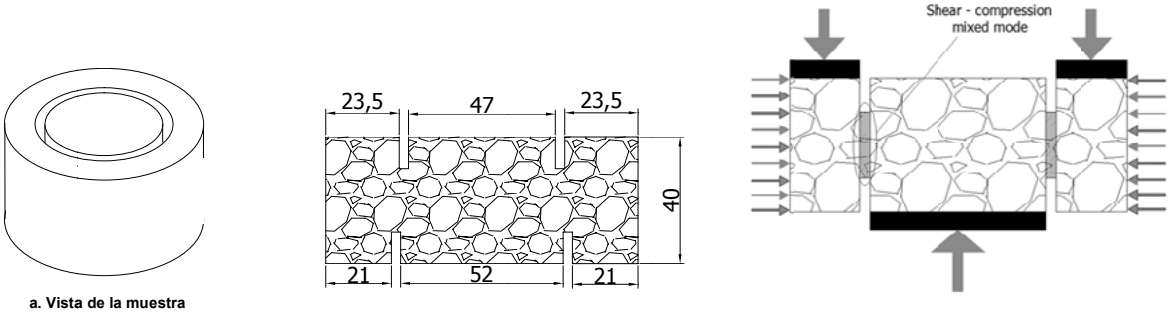

Figure. 1: Specimen geometry and loading.

The top and bottom cylindrical notches are coaxial, 10 mm deep, leaving between them an also cylindrical notch of height 20mm. In order to produce a vertical crack, the upper and lower notches have slightly different diameters (outer diameter of the upper notch equal to inner diameter of the lower notch). The loading scheme on the specimen is shown in Figure 2, including the lateral pressure on the outer surface of the cylinder providing confinement on the fracture plane, and the special platens top and bottom leading to shearing of the ligament surface.

Except for some uniaxial reference tests, lateral confinement is obtained with the large capacity triaxial cell shown in Figure 2 (left). In pressurized tests, specimens are protected with membranes. Specially designed load platens and other elements shown in the figure guarantee post-peak stability of the test and prevent oil penetration along the specimen-platens contact surfaces, etc. Vertical displacements are measured inside the cell via submersible LVDTs, which directly lead to the shear relative displacement along the fracture surface. Circumferential deformations were measured with circumferential chain of invariable length. The lateral pressure was maintained constant during the test by using a pressure accumulator (Figure 2, right). More details of the experimental setup can be found in [4,7].

The test series reported corresponds to conventional concrete with uniaxial strength of 30 MPa, elastic modulus of 25000 MPa and maximum aggregate size of 6 mm. Out of the various test series carried out, the ones used for this simulation include one unconfined test and three confined tests at 2, 4 and 8MPa lateral pressure.

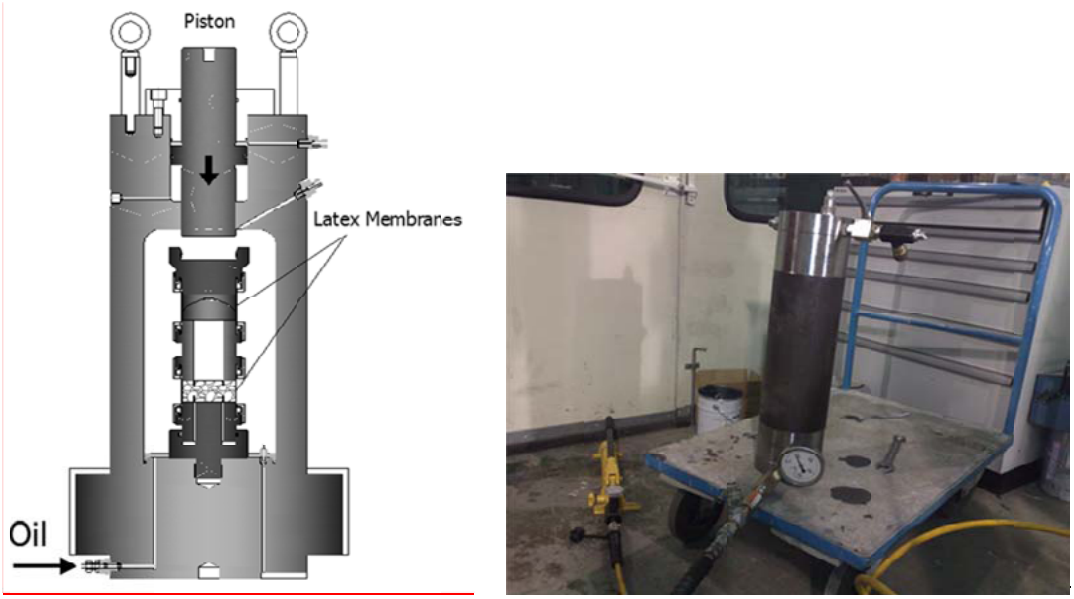

Figure 2: General diagram of confined shear tests (left), and constant pressure cell (right).

The main experimental curves obtained are represented in Figure 6 (rugged curves), together with the computational simulations explained in the next Section (smooth curves). The typical curve of shear stress (vertical force divided by ligament area, minus the force of elastic springs under the external base of specimen) vs. shear relative displacements (vertical displacements), shows an initial elastic response, followed by a peak, softening and residual values. As expected, curves for higher confinement exhibit higher peak and higher residual stress values. The circumferential deformation is also shown in the figures, with dilatancy decreasing for higher confinement pressures, and practically vanishing for the maximum confinement of 8 MPa.

Figures 3 and 4 show the specimens after the test. The tensile radial cracks produced in the unconfined specimen (which are totally developed and in fact the specimen can be physically separated into pieces) are shown in Figure 3 left, while for high confinement, the specimen does not almost crack radially and the inner core of the cylinder slides along the outer shell. (Figure 3, right). Figure 4 depicts the image of a specimen after one of the preliminary tests with a confining pressure of about 4 MPa, which was then cut with a saw in two halves. In the exposed cross-section it can be clearly seen that the fracture plane is produced along an approximately straight line, cutting through the aggregates and matrix as expected. In this specimen tensile radial cracks were not appreciated. These observations strongly suggest that in this case the mode IIa proposed originally as a convenient theoretical/numerical tool [2,8], was in fact practically reached or nearly approached in the experiments. This interpretation is also supported by dilatancy being drastically reduced for tests with confinement of 4MPa, and practically disappearing for 8MPa.

Figure 3: State of specimen after the unconfined test, with large fully developed radial cracks (left), and circumferential cracks with displaced core in a specimen tested under confining pressure of 8 MPa (right).

Figure 4: Fracture plane in confined test specimen, note the displaced aggregate which has been cut through in two pieces by a sensibly straight crack.

4 NUMERICAL MODELING

The FE mesh used for the numerical simulations is represented in Figure 5 (left). Taking advantage of symmetry, one fourth of the specimen is discretized with solid tetrahedral elements. Two main potential cracks are included in the mesh using pre-inserted zero-thickness interface elements: the circumferential ligament, and a radial crack plane extending from the ligament to the outer perimeter. In view of the crack patterns observed in experiments, the latter is introduced along a vertical plane at 45 degrees dividing the discretization in two halves. One of such halves is represented in the right side of Figure 5, showing the cylindrical ligament (in red) and the vertical plane (exposed surface, not colored).

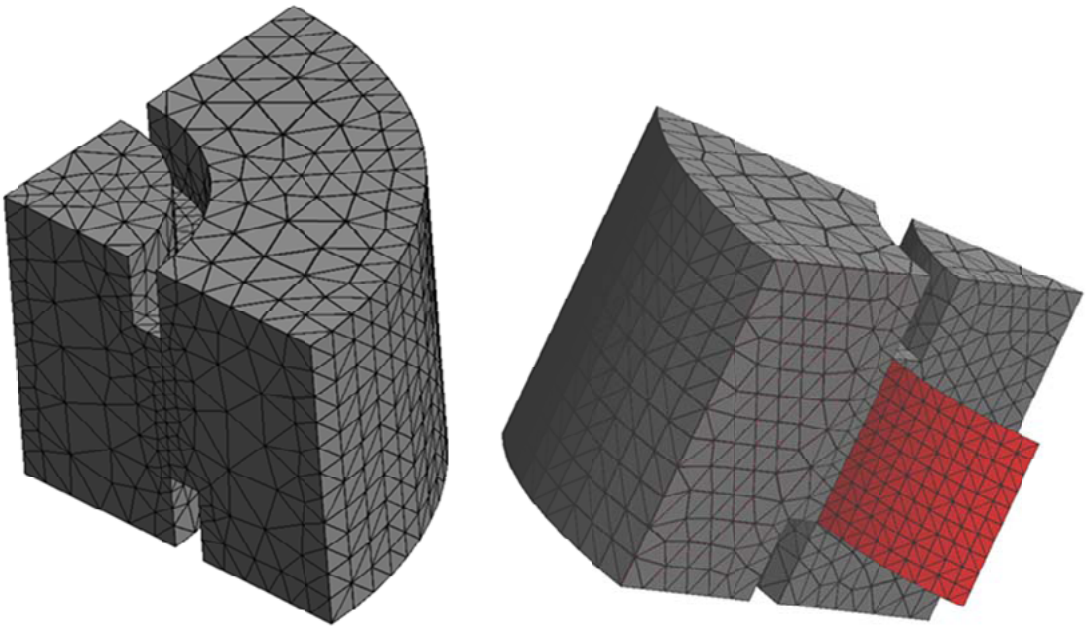

Figure 5: FE mesh (left), and potential fracture planes along which zero-thickness interface elements have been inserted (right): along the cylindrical ligament (in red), and also along the exposed vertical face at 45 degrees.

The continuum elements are assumed linear elastic, while the interface elements are equipped with an elasto-plastic fracture-based constitutive law that incorporates parameters G_f^{I} and G_f^{IIa} as described elsewhere [2]. The preliminary curves obtained after some adjustment, for values of the fracture energies of 0.15 and 12 N/mm, are represented in the same diagram as the experimental results (Figure 6). The calculations exhibit general good agreement with the experimental curves, capturing the essential features (peak values, general shape of curves, dilatancy reduction trends, etc.), although there are still some discrepancies, mainly the post-peak of the unconfined tests, or the still remaining dilatancy for high confinements. Ongoing work is aimed at the final adjustment process.

Additional to the comparison to available experimental data, once adjusted, the model offers extensive additional information that would be very expensive (or sometimes impossible) to obtain from the lab test. In Figure 7, the evolution of the energy spent in the fracture process at each point of both fracture surfaces (ligament and radial plane) is represented by means of color contours. This is done for the three cases of 2, 4 and 8MPa confinement pressure (lower, middle and top) and, for each one, at three stages of the load-displacement curves (peak, middle of descending branch, and residual, from left to right).

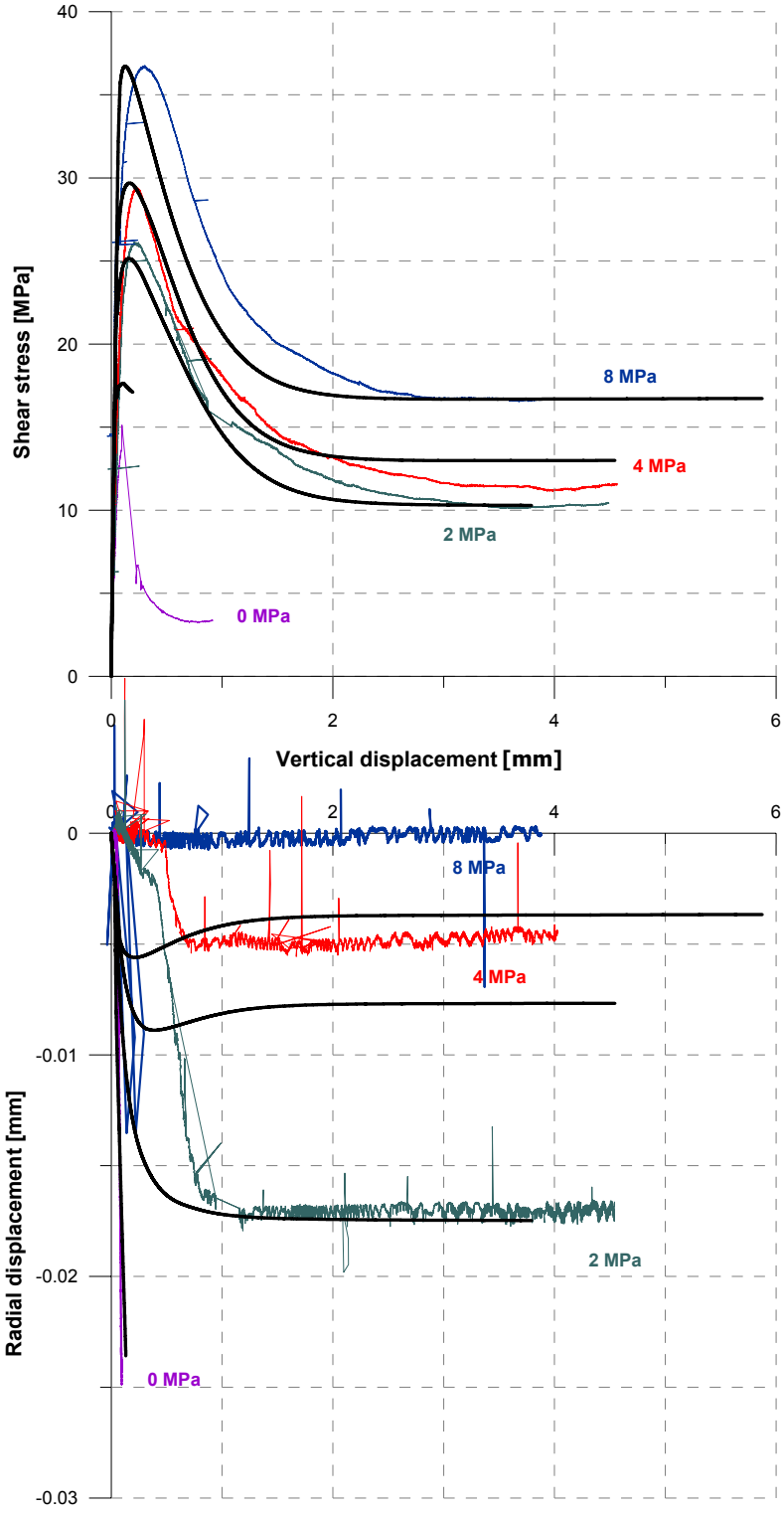

Figure 6: Experimental curves for 2, 4 and 8 MPa confining pressure.

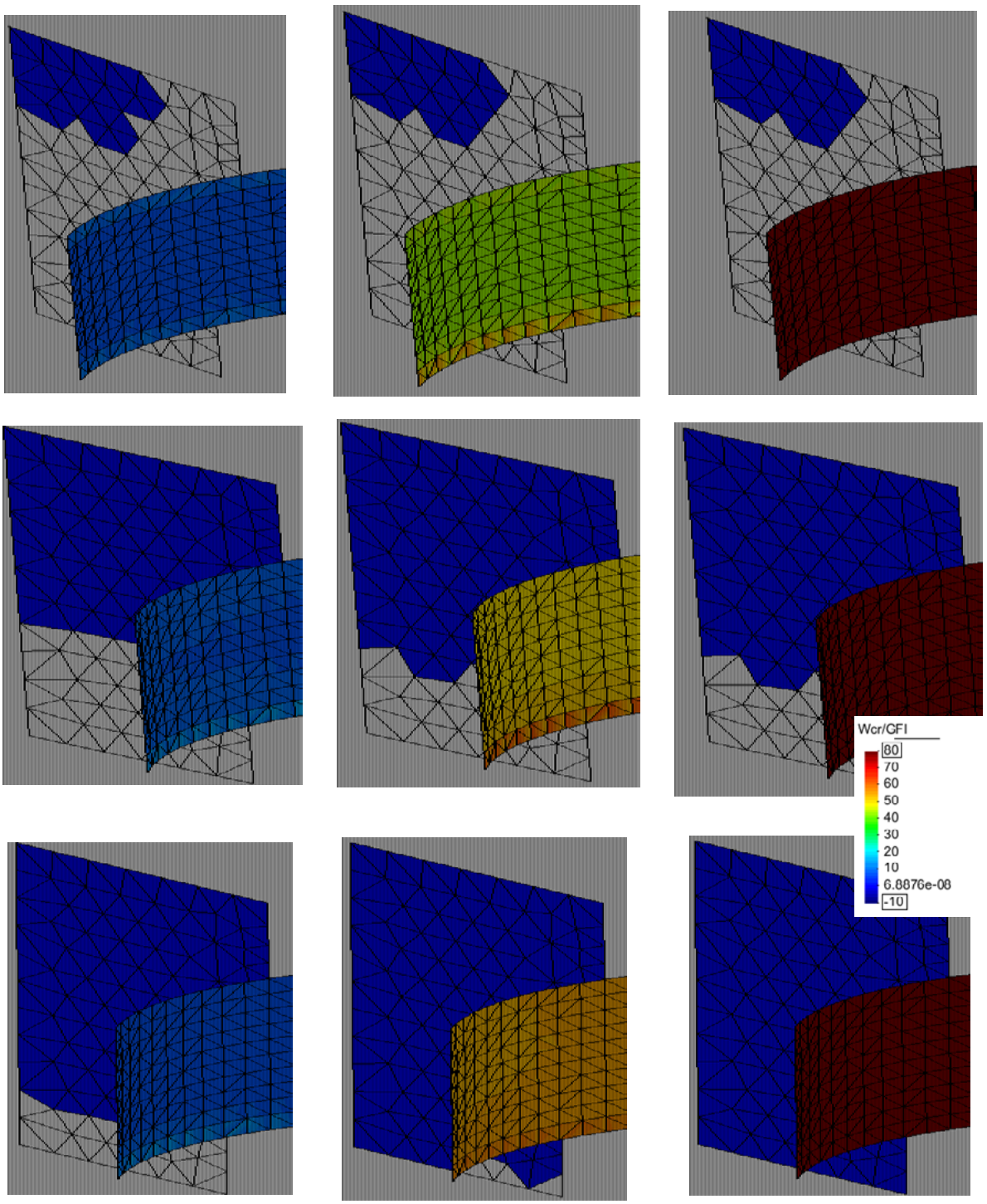

Figure 7: Evolution of dissipated energy on the fracture planes, for confining pressures of 8, 4 y 2 MPa (from top to bottom), and at three stages of the corresponding load-displacement curves of Figure 6: peak loads (left), intermediate point in descending branch (center), and residual state (right).

The figure shows that, for the three cases considered, at the final (residual) state, the normalized energy spent over the ligament Wcr/G_f^{I} approaches the maximum value $G_f^{\mathrm{IIa}}/G_f^{\mathrm{I}}$ in the input data (80). This means that, effectively, the entire ligament is in residual state. Over the entire shear process, the state over the whole ligament seems to develop quite uniformly.

With regard to the radial crack, it is apparent that for the case of higher confinement, in which the dilatancy is lower, only a small portion of this crack is activated, while for lower confinement almost the entire crack is opening. In Figure 8, the state of the radial crack is represented in more detail, with a different scale of colors (maximum value $Wcr/G_f^{\mathrm{I}}=1$, since due to symmetry this cracks opens in pure tension). The lower scale values make it also possible to discriminate among different opening levels in the various areas of the crack plane. Note the negative sign in the lower scale limits, that in the convention used means arrested crack (while the absolute value indicates the amount of energy spent at that point during the loading phases before the current unloading). In the figure, the upper part of specimen clearly shows a more pronounced tensile opening, while the general level of dissipation is much lower than the circumferential ligament, barely reaching the mode I fracture energy G_f^{I} which is anyway the limit value of that can be spent in pure tension before the crack is totally open.

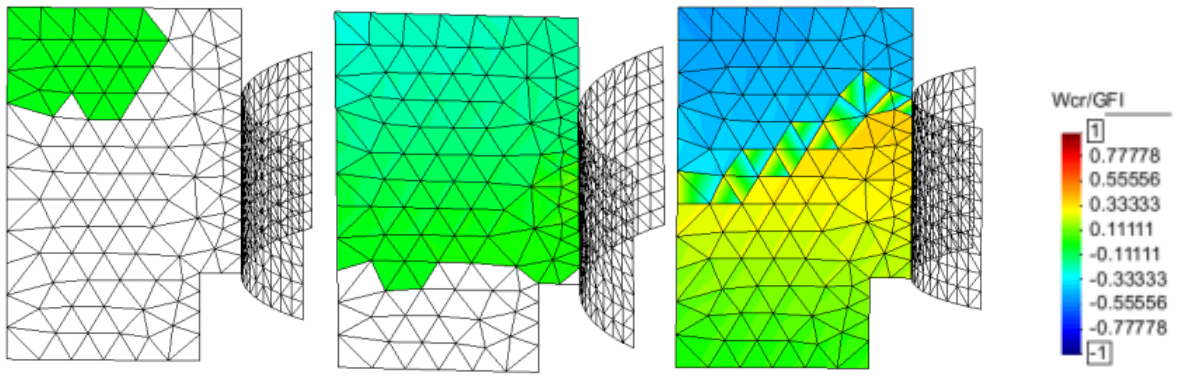

Figure 8: Dissipated energy contours on the radial crack plane in the residual state, for the three confinement levels of 2 (right), 4 (center) and 8 (left) MPa.

5 CONCLUDING REMARKS

Numerical modeling of a confined fracture test for concrete specimens has been presented. The numerical model, representing fracture via zero-thickness interface elements, leads to realistic results, showing the capabilities of this approach to model fracture under a variety of situations. The numerical results obtained turn out useful in this case to understand the stress state occurring in the specimen, and crucial to calibrate the corresponding fracture energy parameter. As important outcomes of the overall study, it is confirmed that a shear-compression crack can be indeed obtained along the pre-determined fracture surface, and that the application of increasing confining pressure seems to leads to the desired mode IIa crack with no dilatancy and associated parameter G_f^{IIa}, as previously predicted in a theoretical context [2].

Acknowledgements

This research has been supported partially by research project BIA2012-36898 funded by MEC (Madrid), which include FEDER funds. Partial support from grant 2009SGR-180 from AGAUR-Generalitat de Catalunya (Barcelona) is also greatly appreciated.

REFERENCES

[1] Carol, I. and Prat, P. Multicrack model based on the theory of multisurface plasticity and two fracture energies. *In E.Oñate et al, eds, COMPLAS4.* CIMNE (UPC) Barcelona, Pp 1583-1594, (1995).

[2] Carol, I., Prat, P. and Lopez, C.M. Normal/shear cracking model: Application to discrete crack analisys. *Journal of Engineering Mechanics.* Vol. 123, No.8, Pp. 765-773, (1997).

[3] Montenegro, O., Carol, I., Sefer,D. Characterization of confined mixed-mode fracture in concrete. In: *Fracture Mechanics of Concrete and Concrete Structures (FRAMCOS 6)*. A. Carpienteri et al., editors. Taylor and Francis. pp, 257-261, (2007a).

[4] Montenegro, O., Sfer, D., Lopez, CM. and Carol, I. Experimental tests and numerical modeling to indentify the asymptotic shear-compression mode IIa of concrete fracture. In *Proc. of the VIII International Conference on Fracture Mechanics of Concrete and Concrete Structures (FraMCoS-8)*, J.G.M. Van Mier, et al. Editors, CIMNE, pp. 271-277, (2013).

[5] Luong, M.P. Tensile and shear strength of concrete and rock. *Engineering Fracture Mechanics.* Vol. 35, Nº1/2/3, pp 127-135, (1990).

[6] Luong, M.P. Fracture testing of concrete and rock materials. *Nuclear Engineering and Design* Vol. 133, pp 83-95, (1992).

[7] Montenegro, O., Sfer, D., Carol, I. Characterization of concrete in mixed mode fracture under confined conditions. *In Gdoutos, E.E., editor, Experimental analysis of nano and engineering material and structures,* pp. 1–8. Springer. (Proc. of the 13th Int. Conf., Alexandroupolis, Jul/1-6/2007) – in CD-ROM, (2007b).

[8] Carol , I. and Prat, P. A statically constrained microplane model for the smeared analysis of concrete cracking. *In N.Bicanic and H. Mang, eds, Computer-Aided Analysis and Design of Concrete Structures (Proc. Sci-C 1990),* Pineridge Press, pp 919-930, (1990).